

Towards Fine-grained Visual Representations by Combining Contrastive Learning with Image Reconstruction and Attention-weighted Pooling

Jonas Dippel
jonas.dippel@bayer.com
Bayer AG
Berlin, Germany

Steffen Vogler
steffen.vogler@bayer.com
Bayer AG
Berlin, Germany

Johannes Höhne
johannes.hoehne@bayer.com
Bayer AG
Berlin, Germany

Abstract

This paper presents Contrastive Reconstruction, ConRec - a self-supervised learning algorithm that obtains image representations by jointly optimizing a contrastive and a self-reconstruction loss. We showcase that state-of-the-art contrastive learning methods (e.g. SimCLR) have shortcomings to capture fine-grained visual features in their representations. ConRec extends the SimCLR framework by adding (1) a self-reconstruction task and (2) an attention mechanism within the contrastive learning task. This is accomplished by applying a simple encoder-decoder architecture with two heads. We show that both extensions contribute towards an improved vector representation for images with fine-grained visual features. Combining those concepts, ConRec outperforms SimCLR and SimCLR with Attention-Pooling on fine-grained classification datasets.

1 Introduction

Recent advances in the field of self-supervised learning have shown exciting progress. For the first time, He et al. [18] have reported that the concept of contrastive learning applied in unsupervised pretraining can outperform supervised pretraining used in several computer vision tasks. Additional corroborating reports [23, 28, 32] followed, which confirmed the notion that contrastive learning indeed leads to a representation that is well suited for challenges such as few-shot classification or domain transfer. The combination of unsupervised pretraining with supervised fine-tuning is especially attractive for many real-world application because it provides a solution to the common issue of shortage of labeled data [2, 10, 20, 36]. Large amounts of unlabeled, task-agnostic data could be leveraged to create a representation that get subjected to supervised fine-tuning using fewer labeled data [7].

Whether representations gained with contrastive learning are suitable for fine-grained classification still needs to be studied as this kind of tasks poses a harder challenge due to subtlety of required attributes. Fine-grained classification tasks are characterized by intra-class variations being potentially greater than the inter-class variations [33]. In practice, a high degree of similarity among categories can be observed and large numbers of attributes are required to effectively

model these subtle differences. Moreover, only the combination of multiple sub-regions within an image might be predictive for the class [13]. In contrast, the entire image can be subject to confounding effects including different viewing angles, lighting, or partial occlusion [17, 33]. Therefore, a fine-grained classifier needs to be able to interpret fine scale features in presence of coarse scale perturbations (notably, these coarse perturbations could hold predictive value themselves). Therefore, such tasks pose a challenge to models which utilize representations derived via unsupervised pretraining.

We exemplified these shortcomings by showing that the image representations obtained through SimCLR [6, 7] lead to inaccurate model performance in a carefully designed synthetic dataset for fine-grained classification.

Further, we found that the addition of an attention pooling mechanism and a self-reconstruction loss successfully addresses this limitation. Moreover, we present a novel approach that utilizes a combination of contrastive learning and a self-reconstruction task. The proposed learning paradigm yields improved performance in multiple fine-grained classification tasks, which confirms that the combination of a contrastive loss and a self-reconstruction loss leads to representations of sufficiently high granularity.

We hope this provides further understanding to future efforts to build representation that can be applied across a wide range of domains and tasks.

2 Method

The core concepts of ConRec are depicted in Figure 1. Starting with N unlabeled images \mathbf{x} , we generate 2 augmented images for each input image, which yields $2N$ augmented images $\mathbf{x}_i, i \in \{1..2N\}$ that serve as reconstruction targets. The ConRec model receives an artificially masked image $\tilde{\mathbf{x}}_i$ with the task to reconstruct \mathbf{x}_i . For each input $\tilde{\mathbf{x}}_i$, ConRec also outputs contrastive representations \mathbf{z}_i which are optimized to be similar (dissimilar), if the inputs i and j originate from the same (from a distinct) unlabeled image.

2.1 Model Architecture

The ConRec model is a deep neural network with one input and two outputs. The model architecture can be divided

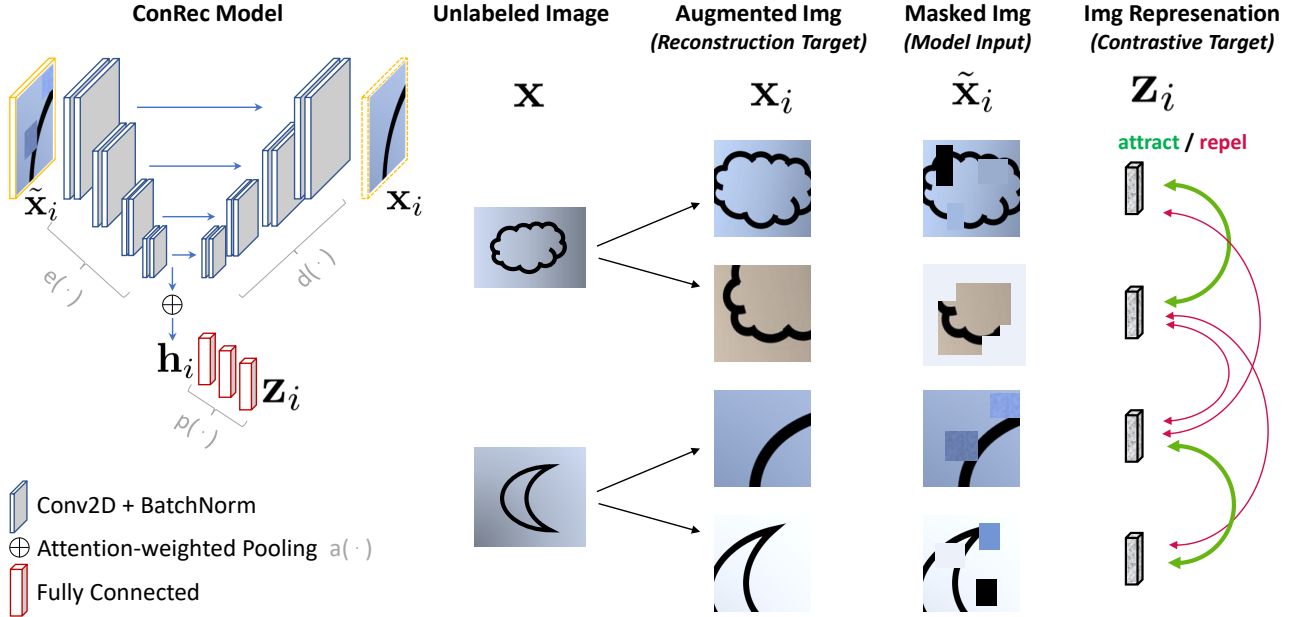


Figure 1. Learning Framework for Contrastive Reconstruction – ConRec. The ConRec model consists of a fully convolutional encoder-decoder architecture with skip connections as well as a projection head comprising fully connected layers. The model receives a masked image \tilde{x}_i and outputs the unmasked reconstruction target x_i as well as the contrastive image representation vector z_i . For a batch of N unlabeled images, the model receives $2N$ masked-augmented images and simultaneously performs a reconstruction task and a contrastive task. Within the contrastive task, representations z_i and z_j are optimized to be similar (dissimilar), if the inputs i and j arise from the same (from a distinct) original image.

into four components: encoder $e(\cdot)$, decoder $d(\cdot)$, attention-weighted pooling $a(\cdot)$ and projection head $p(\cdot)$ as shown in Figure 1. We chose the U-net [27] as the main backbone for the encoder and decoder for ConRec. In the training process, the model receives a masked image \tilde{x}_i and outputs the reconstructed image $x_i = d(e(\tilde{x}_i))$ as well as the contrastive vector representation $z_i = p(a(e(\tilde{x}_i)))$. The training loss is composed of two parts: the contrastive loss L_c and the reconstruction loss L_r .

$$L_{ConRec} = L_c + \alpha * L_r \quad (1)$$

Reconstruction loss L_r assesses the reconstruction quality through the pixel-wise mean squared error between the predicted reconstruction and the ground truth image.

$$L_r = \frac{1}{N} \sum_i^N (d(e(\tilde{x}_i)) - x_i)^2. \quad (2)$$

Following the SimCLR framework, we use the normalized temperature-scaled cross entropy loss (NT-Xent) as contrastive loss L_c with

$$L_c^{(i,j)} = -\log \frac{\exp(\text{sim}(z_i, z_j) / \tau)}{\sum_{k=1}^{2N} \mathbb{1}_{[k \neq i]} \exp(\text{sim}(z_i, z_k) / \tau)} \quad (3)$$

where τ depicts the temperature parameter. We refer to Algorithm 1 in Chen et al. [6] for a precise description of loss term L_c .

After the training is completed, we discard the projection head and the decoder and we only use the encoder $e(\cdot)$ and the attention pooling $a(\cdot)$ to generate image representations with $h_i = a(e(x_i))$.

2.2 Augmentation

Two types of augmentations are applied to the image. First, we apply the augmentations from SimCLR [6] including cropping, color jitter and blurring. Then, we apply augmentations that have to be reversed by the reconstruction task as described in [38]. These augmentations include in-painting, where a randomly sized rectangle is placed on the image, out-painting where the outer parts of the image are masked and local-pixel shuffling where the pixels in a region of the image are shuffled. In the case of single channel images, we also apply non-linear transformations (see [38]). The unmasked image is then used as a target for the reconstruction task. Figure 3 shows augmentation examples and the respective reconstruction predictions by our model.

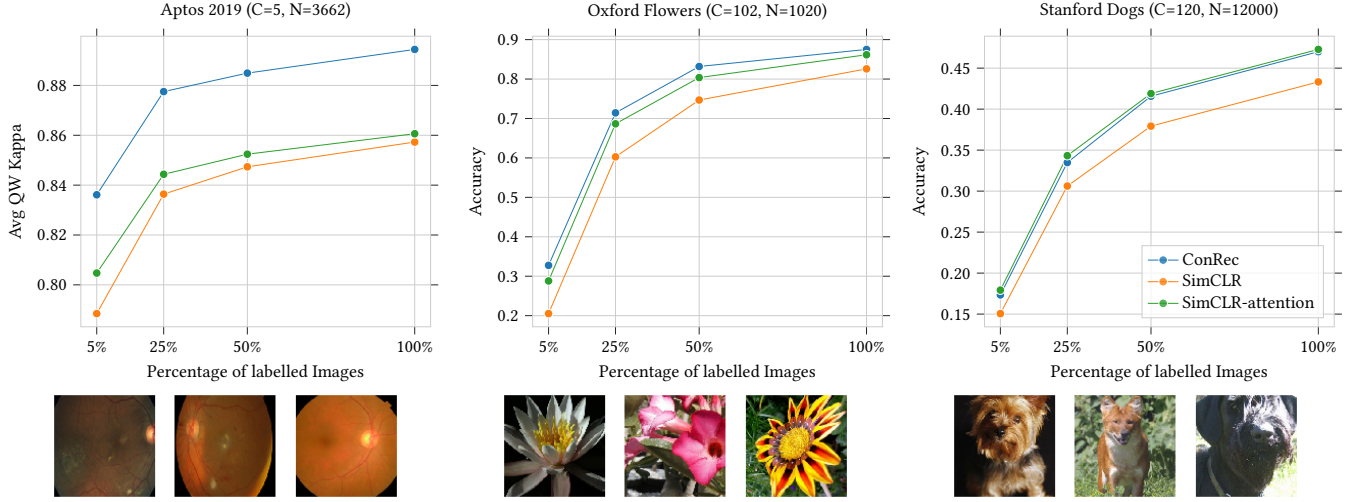


Figure 2. Model accuracies for various amounts of labels. Each representation model was trained on all available training data and a linear classifier was trained on a subset (1% to 100%) of the labeled representations. All metrics were computed on the same fixed test data. This experiment was conducted for three datasets with different number of classes C and number of samples N . The top row depicts the validation metric of the linear model. Sample images from the dataset are shown below.

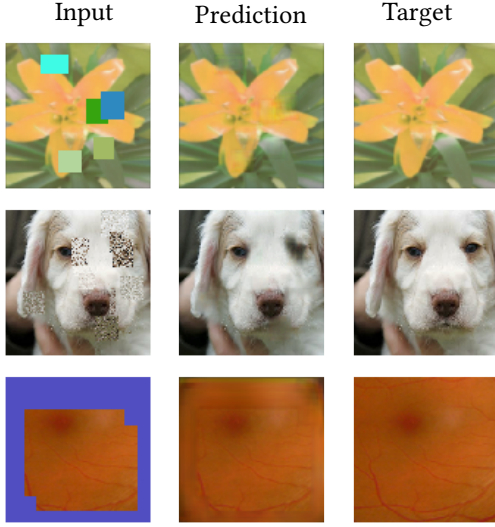


Figure 3. Augmented images and respective reconstruction predictions by our ConRec model. The images were selected from the Oxford Flowers, Stanford Dogs and Aptos 2019 dataset, ordered top to bottom. In-painting is shown in the first row, the second row shows local-pixel-shuffling and the last one image-out-painting.

2.3 Attention-weighted Pooling

SimCLR [6] uses global average pooling at the output of the encoder to reduce the dimensionality before the dense layers in the projection head. This pooling operation discards some

local features in the output activation map, which may carry relevant fine-grained information.

We introduce an attention weighted pooling mechanism that aggregates the spatial content of the final feature map of the encoder in a parametric manner. This spatial weighting yields an improved image representation \mathbf{h} which is then fed into the projection head.

Suppose, we have an encoder output activation map $\phi \in \mathbb{R}^{w \times h \times f}$. First, we compute an attention weight a_{ij} for each location $(i, j) \in \mathbb{N}^{w \times h}$. This is done by applying three consecutive convolution blocks (convolution, batch norm, ReLU activation) with decreasing number of filters and then one final convolution with one filter (sigmoid activation). The weights and biases of the four convolutions are trainable with the end-to-end model. By replicating a_{ij} across dimension f , we obtain a matrix $A_\phi \in \mathbb{R}^{w \times h \times f}$. The final pooling output $a(\phi) \in \mathbb{R}^f$ is then computed as following:

$$a(x) = g(A_\phi \odot \phi) \odot \frac{1}{g(A_\phi)} \quad (4)$$

where g denotes standard 2D global average pooling. Note that the attention-weighted pooling is only applied in the contrastive head. In analogy to our approach, Radford et al. [26] also recently proposed a self-attention pooling mechanism as part of their CLIP model.

2.4 Implementation Details

In contrast to the large mini batches from SimCLR, we use a batch size of 16 resulting in a true batch size of 32 and perform model training on a single Volta V100 GPU with 16GB memory. Given the small batch size, the convergence time

of SimCLR is increased. Furthermore, compared to SimCLR, ConRec has an additional decoder which yields an increased model size and an increased training time by factor 2. For the results in Section 4, pretraining of the ConRec U-net model needed 270k - 900k training steps (depending on the dataset size) which results in infrastructure costs of 156 - 506\$¹ per model training. Our implementation is available on Github². We reuse the parameters for pretraining on ImageNet. In detail, we use the LARS Optimizer with a constant learning rate of 0.3, weight decay of 10^{-4} and color jitter strength of 1.0. Furthermore, we use a temperature value of 0.5 which yielded better results than a temperature value of 0.1 for our datasets. To achieve the same magnitude in the loss terms, we use a factor of $\alpha = 100$ for the reconstruction loss.

2.5 Evaluation Protocol

To separately show the effect of our attention mechanism and the reconstruction task, we compare the performance of ConRec with the SimCLR framework implementation [6] using standard global average pooling (SimCLR) and with the attention-weighted pooling mechanism (SimCLR-attention). For each method and dataset, we pretrain the model on the training set. After pretraining, we compute the representations of each image in the training and test set and use center-cropping if the images are not of the same size. For evaluation, a logistic regression classifier is trained on the representations of the training set and then evaluated on the representations of the test set. During pretraining, we evaluate our model every 20 epochs and choose the best performing model for final evaluation.

3 Pretest using Synthetic Dataset

We designed two synthetic datasets in order to assess performance of representation learning methods for classification tasks that require fine-grained image representations. This test bed enables to directly compare the linear classifiability of image representation from several methods. The two test scenarios are tailored to simulate data environments in which class discriminant information is either captured in a very fine-grained local feature or a holistic scene view – see Figure 4. On a general note, we are aware that there are no well-defined criteria to distinguish fine-grained classification scenarios from other image classification tasks that require holistic image representations. In an attempt to probe these concepts, we designed two synthetic datasets, which are basis for the following experiment.

We find that the image representations provided through a contrastive task (i.e. SimCLR) are well suited for the holistic scenario but they are not well suitable to exploit fine-grained details. In contrast, the image representations provided through a reconstruction task fall short for the holistic scenario, but they capture the fine-grained visual features. Image representations provided through ConRec are well suited for both scenarios – see Table 1.

3.1 Rationale of the Design

Rectangle-Triangle - We generate images that contain a rectangle with either right or round corners and a triangle, which is either equilateral or right-angled and placed inside the rectangle. By combining these two properties of each geometric object, we obtain four classes in total. In this case, multiple, disjoint low-level details in the images (angles in the triangle and shape of the rectangle corners) are important features for the classification. This favors approaches that generate fine-grained representations.

Circles-Square - We generate images that contain either two circles (class 1), a square and a circle (class 2), or two squares (class 3). For this task, it is not sufficient to represent the image exclusively through local information such as the edge of a single object. Instead, the representations must capture the identity and relation between the two objects and thus non-local information in order to be discriminative for the classification problem. This is what we refer to as *holistic information* in an image.

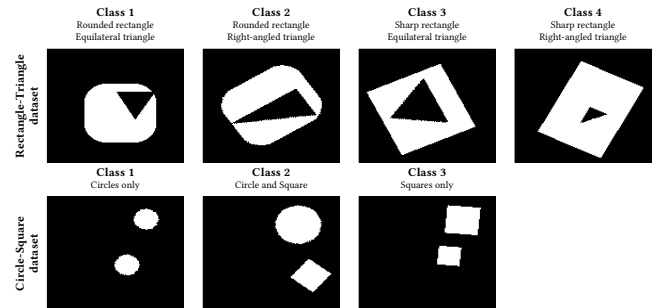


Figure 4. Representative examples of two synthetic datasets. All samples from the datasets were generated as binary images with 128x128 pixels. Size and position of individual objects is subject to randomization, whereas overall design is determined by code.

3.2 Results

For each dataset, we generated a training and a test set with 1000/500 samples for the Rectangle-Triangle and 600/400 samples for the Circle-Square dataset. During pretraining, we evaluate the model’s representations every 20 epochs

¹on a AWS p3 instance with costs of 4,22\$ per hour

²<https://github.com/bayer-science-for-a-better-life/contrastive-reconstruction>

and report the best results for each method after training for 1000 epochs in Table 1.

The results on the *Rectangle-Triangle* dataset reveal that the model trained on the reconstruction task outperforms SimCLR and SimCLR-attention. Thus, the contrastive loss is not able to capture the fine-grained visual details in the representations. ConRec is able to capture these details and outperforms all other approaches.

On the *Circle-Square* dataset, SimCLR and SimCLR-attention clearly outperform the reconstruction task. Due to the holistic design of the dataset, this indicates that the reconstruction task is not well suited to create a corresponding representation of the image. It further suggests that the reconstruction task has its strength at encoding fine-grained features into the representations. In comparison, ConRec is capable to produce representations with holistic information and therefore almost reaches the performance of the two SimCLR variants.

To conclude, the synthetic dataset results exemplify that ConRec is able to exploit both a holistic representation as well as fine-grained visual details of an image. Additional research is needed to assess the importance of individual reconstruction losses as our current implementation, the MSE, is known to have limitations [25].

Table 1. Linear evaluation accuracy on two synthetic datasets. The Rectangle-Triangle dataset requires local features and the Circles-Squares a holistic view on the image for good classification performance.

Method/Dataset	Rectangle-Triangle	Circles-Squares
SimCLR	85.6	99.50
SimCLR-attention	90.4	99.50
Reconstruction	91.8	86.47
ConRec with GA Pool	93.4	99.50
ConRec	96.4	98.75

4 Benchmark Classification Tasks

We evaluate our method on two publicly available fine-grained classification tasks and one medical dataset following our evaluation protocol described in Section 2.5. We pretrain until convergence of the linear evaluation performance. This results in 1200 / 2700 / 1200 training epochs for the Aptos 2019 / Oxford Flowers / Stanford Dogs dataset respectively. The evaluation performance during pretraining is depicted in Figure 5. Final evaluation results with various training subsets are shown in Figure 2. Furthermore, we compare our linear evaluation results with other baselines in Table 2. We evaluate an ImageNet pretrained DenseNet121 with logistic regression in the same fashion as our pretrained models. Furthermore, we trained our U-net model (with standard global average pooling) and a DenseNet121 from scratch

and report classification accuracy on the test set. For the linear evaluation results in Table 2, we additionally use crop augmentations when training the linear classifier which results in improved classification performance for the Stanford Dogs and Oxford Flowers dataset.

Comparing the results of models with self-supervised pretraining and a frozen encoder to models trained with a random initialization, the general benefit of using self-supervised pretraining becomes apparent. However, using the ConRec framework achieves the best results across all datasets except Stanford Dogs where it is en par with SimCLR-attention.

We explicitly report the linear performance results only and did not do any finetuning of the encoder, since the impact of self-supervised pretraining can be best evaluated in the linear evaluation regime [6].

4.1 Oxford Flowers

The Oxford Flowers dataset consists of 102 classes of flowers. Similar to Chen et al. [6], we use the official train and validation split combined as the training set which contains 20 images per class resulting in 2040 total images. For evaluation, we use the official test split with 6,149 samples.

The results show that the attention mechanism helps to improve the representations of the SimCLR framework across all subsets. The reconstruction task additionally improves the representations by a significant margin. Especially in low data regimes, the performance gain increases.

4.2 Diabetic Retinopathy Classification (Aptos 2019)

We also evaluate all models on a medical dataset where fine grained details are often important for classification performance. We use the Aptos 2019 Kaggle Challenge [1] which also has been studied in the context of self-supervised learning by Taleb et al. [31]. As the labels of the test set are not public, we follow their approach and evaluate our models with 5-fold cross validation on the training set. The evaluation metric in this case is the average weighted quadratic kappa. Our results show that the attention mechanism only moderately increases the performance in this case. However, the addition of the reconstruction task results in a significant performance gain.

Welikala et al. [34, 35] perform extensive feature engineering for diabetic retinopathy detection. They show that the morphology of the local retinal vasculature is important for classification performance. We suppose that this are local features that can be better captured by the reconstruction task and therefore result in an increased linear performance.

We also investigated, if the reduced batch size is a limiting factor of our SimCLR implementation. Therefore, we pre-trained the SimCLR implementation with batch sizes 4, 8, 16, 32 and 64 and show the average linear performance during pretraining in Figure 6. The results show that although the performance significantly increases from batch size 4 to 8, an

Table 2. Linear evaluation results and respective baselines. For the Aptos 2019 dataset, the evaluation metric is the average quadratic weighted kappa after performing 5-fold cross validation on the training set. For all other datasets, categorical accuracy on the test set is reported. ImageNet results in parenthesis indicate flaws in the evaluation as the datasets were included in supervised ImageNet-pretraining.

Model	Frozen Encoder	Aptos 2019	Oxford Flowers	Stanford Dogs	#Parameters
SimCLR U-net	✓	85.72	86.01	43.96	4.693M
SimCLR Attention U-net	✓	86.06	88.37	50.31	4.867M
ConRec U-net	✓	89.44	90.29	49.57	4.867M
DenseNet121 (ImageNet Init)	✓	86.70	(92.97)	(88.07)	8.062M
U-net (Random Init)		82.11	81.54	55.2	4.693M
DenseNet121 (Random Init)		64.53	82.03	57.63	8.062M

additional batch size increase does not result in a significant performance gain.

Comparing our results to Taleb et al. [31], we achieve significantly higher quadratic weighted kappa score while only using the training data from the Kaggle Challenge during pretraining and performing linear evaluation on the representations as opposed to finetuning the whole model.

Furthermore, ConRec’s representations also outperform the representations of an ImageNet-pretrained DenseNet121. This highlights the benefits of in-domain pretraining rather than transferring from pretrained models that were trained on large out-of-domain datasets. This confirms both the initial observation by He et al. [19] stating that ImageNet-pretraining does not necessarily lead to better performance in other tasks and also Ke et al. [22], which shows that ImageNet performance does not correlate with performance on fine-grained classification of medical images (specifically CheXpert in this example).

4.3 Stanford Dogs

The Stanford Dogs dataset contains images of 120 breeds of dogs and has been built using images and annotation from

ImageNet. The official train set contains 100 images per class resulting in a train set with 12000 images. For evaluation, we use the official test split with 8580 samples.

The results show that the attention mechanism improves the representations for this dataset. However, in contrast to the two other datasets, the addition of the reconstruction task does not result in any performance improvement and ConRec performs equally to SimCLR-attention.

It should be noted that all self-supervised representations are also significantly outperformed by the ImageNet-pretrained DenseNet121. This margin can be explained by the fact that this dataset is a subset of the ImageNet dataset and therefore, the DenseNet121 was exposed to further dog images and true label information during pretraining.

5 Future Work

Due to computational limitations, we were unable to pre-train our model on the ImageNet dataset. This would allow us to compare our representations with other recent advancements in the self-supervised learning space and could help

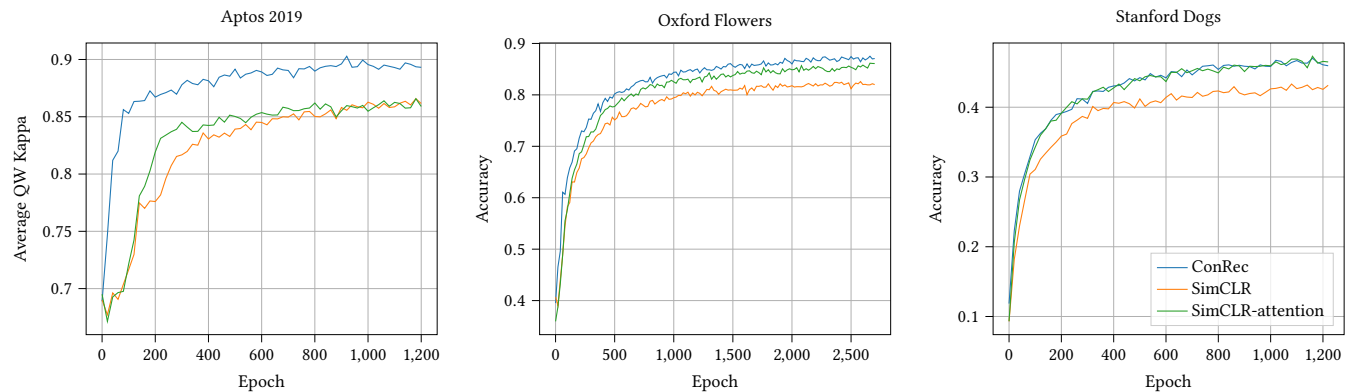


Figure 5. Linear evaluation performance during pretraining using three selected benchmark datasets. The models were evaluated every 20 epochs by fitting a logistic regression classifier on the image representations of the training data and then reporting classification metrics on fixed test data.

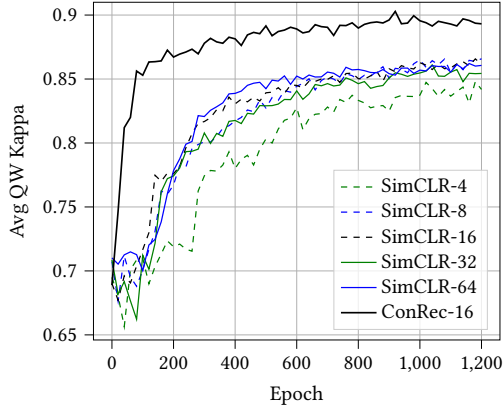


Figure 6. SimCLR pretraining performance on our U-net encoder using standard global average pooling on the Ap-
tos2019 dataset for batch sizes 4, 8, 16, 32, 64 in comparison
to ConRec with batch size 16.

to further study the transferability of the learned representations. Furthermore, adding a decoder increases the memory need. Therefore, a momentum encoder combined with memory bank techniques as presented in MoCo [18] could potentially improve our method. The addition of an adversarial loss which has shown to produce sharper reconstruction predictions [21, 25] could also help to capture even more fine-grained features in the image. Chen et al. [7] showed that intermediate layers in the projection head may build better representations in low data regimes. In our experiments, the representations at the encoder output outperformed the ones in the projection head. Future work should investigate the design of the projection head in combination with the attention mechanism and a reconstruction task. We focused on a U-net architecture [27] for pretraining our models. Further research should also investigate if our self-supervised model pretraining can be beneficial for segmentation tasks as it was shown for other reconstruction-based approaches [25].

6 Related Work

Self-supervised learning methods aim to construct semantically meaningful representations in the absence of labels or any semantic annotations. Self-supervised learning has been widely studied for several domains such as image [23], audio [29] or multiple modalities [24, 26, 30]. Three types of learning tasks are commonly used for self-supervised learning in computer vision tasks. Models trained with handcrafted pretext tasks predict properties of an image such as colorization [37], rotation [14], or patch relatedness [11].

Self-reconstruction tasks let the model learn to reconstruct an artificially corrupted input. A simple but successful self-reconstruction approach is the in-painting task [25] where the model generates the content of an arbitrary image patch

conditioned on its surrounding. In Model Genesis [38] this concept was extended to 3D medical images and the model restores the complete image while parts of the input were occluded. In the Parts2Whole approach [12], the model learns part-whole semantics by reconstructing a whole (i.e. a 3D image) from its parts (i.e. several 3D crops). Due to the generative nature of the task, self-reconstruction models are commonly implemented as encoder-decoder architectures, which make them suitable for transfer learning in segmentation problems [25].

For contrastive learning tasks, the model aims to generate a representation that maximizes the similarity between positive pairs while minimizing the similarity between negative pairs. In visual representation learning, positive/negative pairs are commonly generated by sampling two patches from the same/different image. Multiple approaches for contrastive image representation have recently been proven successful: SimCLR [6, 7] provides a simple learning framework that allows to sample negative pairs within each mini batch. Therefore, SimCLR benefits from larger batch sizes and it can be trained without a memory bank of negative pairs. Having a similar learning target, Momentum Contrast [8, 18] can be trained with smaller batch sizes as it keeps a buffer of negatives for loss calculation.

Other recent self-supervised learning approaches also omit extensive negative mining. SwAV [3] uses a clustering-based approach enforcing consistency between cluster assignments produced for different augmentations of the same image. BYOL [15] trains an online network to predict the target network’s representation of the same image under a differently augmented view while updating the target network with a momentum term. Image GPT [5] learns image representations by completing masked images in an autoregressive fashion with a transformer model.

Instead of contrasting two augmentations from the same image, CLIP [26] learns to correctly align images to their corresponding captions. After training on 400 million (image, text) pairs, the model achieves SOTA image representations and enables zero-shot transfer of the model to downstream tasks.

Attention mechanisms were used in other approaches to tackle fine-grained classification: Han et al. [16] introduce an Attribute-Aware Attention Model which uses additional attribute information about the image combined with category label information to build more discriminate feature representations. Chang et al. [4] utilizes a channel-wise attention mechanism which forces all feature channels belonging to the same class to be discriminative across the network. Chen et al. [9] shuffles regions of the input image and trains a region alignment network to restore the original spatial layout.

7 Conclusion

We showcased that the SimCLR framework has shortcomings to capture fine-grained features in its representations. To address this issue, we introduced an attention pooling mechanism and a reconstruction task. On two fine-grained classification datasets and one medical dataset, the attention pooling mechanism improves self-supervised learning performance significantly. The addition of the reconstruction task yields a further performance increase for diabetic retinopathy classification and on the Oxford Flowers dataset.

References

- [1] Aptos 2019 Kaggle Challenge 2019. <https://www.kaggle.com/c/aptos2019-blindness-detection/>. [Online; accessed 15-December-2020].
- [2] Jinkun Cao, Hongyang Tang, Hao-Shu Fang, Xiaoyong Shen, Cewu Lu, and Yu-Wing Tai. 2019. Cross-domain adaptation for animal pose estimation. In *Proceedings of the IEEE/CVF International Conference on Computer Vision*. 9498–9507.
- [3] Mathilde Caron, Ishan Misra, Julien Mairal, Priya Goyal, Piotr Bojanowski, and Armand Joulin. 2020. Unsupervised learning of visual features by contrasting cluster assignments. *Advances in Neural Information Processing Systems* 33 (2020).
- [4] Dongliang Chang, Yifeng Ding, Jiyang Xie, Ayan Kumar Bhunia, Xiaoxu Li, Zhanyu Ma, Ming Wu, Jun Guo, and Yi-Zhe Song. 2020. The devil is in the channels: Mutual-channel loss for fine-grained image classification. *IEEE Transactions on Image Processing* 29 (2020), 4683–4695.
- [5] Mark Chen, Alec Radford, Rewon Child, Jeffrey Wu, Heewoo Jun, David Luan, and Ilya Sutskever. 2020. Generative pretraining from pixels. In *International Conference on Machine Learning*. PMLR, 1691–1703.
- [6] Ting Chen, Simon Kornblith, Mohammad Norouzi, and Geoffrey Hinton. 2020. A simple framework for contrastive learning of visual representations. *arXiv preprint arXiv:2002.05709* (2020).
- [7] Ting Chen, Simon Kornblith, Kevin Swersky, Mohammad Norouzi, and Geoffrey E Hinton. 2020. Big self-supervised models are strong semi-supervised learners. *Advances in Neural Information Processing Systems* 33 (2020).
- [8] Xinlei Chen, Haoqi Fan, Ross Girshick, and Kaiming He. 2020. Improved baselines with momentum contrastive learning. *arXiv preprint arXiv:2003.04297* (2020).
- [9] Yue Chen, Yalong Bai, Wei Zhang, and Tao Mei. 2019. Destruction and construction learning for fine-grained image recognition. In *Proceedings of the IEEE/CVF Conference on Computer Vision and Pattern Recognition*. 5157–5166.
- [10] Olivier Dehaene, Axel Camara, Olivier Moindrot, Axel de Lavergne, and Pierre Courtiol. 2020. Self-Supervision Closes the Gap Between Weak and Strong Supervision in Histology. *arXiv preprint arXiv:2012.03583* (2020).
- [11] Carl Doersch, Abhinav Gupta, and Alexei A Efros. 2015. Unsupervised visual representation learning by context prediction. In *Proceedings of the IEEE international conference on computer vision*. 1422–1430.
- [12] Ruibin Feng, Zongwei Zhou, Michael B Gotway, and Jianming Liang. 2020. Parts2Whole: Self-supervised Contrastive Learning via Reconstruction. In *Domain Adaptation and Representation Transfer, and Distributed and Collaborative Learning*. Springer, 85–95.
- [13] Jianlong Fu, Heliang Zheng, and Tao Mei. 2017. Look closer to see better: Recurrent attention convolutional neural network for fine-grained image recognition. In *Proceedings of the IEEE conference on computer vision and pattern recognition*. 4438–4446.
- [14] Spyros Gidaris, Praveer Singh, and Nikos Komodakis. 2018. Unsupervised representation learning by predicting image rotations. *arXiv preprint arXiv:1803.07728* (2018).
- [15] Jean-Bastien Grill, Florian Strub, Florent Altché, Corentin Tallec, Pierre Richemond, Elena Buchatskaya, Carl Doersch, Bernardo Avila Pires, Zhaohan Guo, Mohammad Gheshlaghi Azar, et al. 2020. Bootstrap your own latent—a new approach to self-supervised learning. *Advances in Neural Information Processing Systems* 33 (2020).
- [16] Kai Han, Jianyuan Guo, Chao Zhang, and Mingjian Zhu. 2018. Attribute-aware attention model for fine-grained representation learning. In *Proceedings of the 26th ACM international conference on Multimedia*. 2040–2048.
- [17] Bijan Haney and Alexander Lavin. 2020. Fine-Grain Few-Shot Vision via Domain Knowledge as Hyperspherical Priors. *arXiv preprint arXiv:2005.11450* (2020).
- [18] Kaiming He, Haoqi Fan, Yuxin Wu, Saining Xie, and Ross Girshick. 2020. Momentum contrast for unsupervised visual representation learning. In *Proceedings of the IEEE/CVF Conference on Computer Vision and Pattern Recognition*. 9729–9738.
- [19] Kaiming He, Ross Girshick, and Piotr Dollár. 2019. Rethinking imagenet pre-training. In *Proceedings of the IEEE/CVF International Conference on Computer Vision*. 4918–4927.
- [20] Sina Honari, Pavlo Molchanov, Stephen Tyree, Pascal Vincent, Christopher Pal, and Jan Kautz. 2018. Improving landmark localization with semi-supervised learning. In *Proceedings of the IEEE Conference on Computer Vision and Pattern Recognition*. 1546–1555.
- [21] Phillip Isola, Jun-Yan Zhu, Tinghui Zhou, and Alexei A Efros. 2017. Image-to-image translation with conditional adversarial networks. In *Proceedings of the IEEE conference on computer vision and pattern recognition*. 1125–1134.
- [22] Alexander Ke, William Ellsworth, Oishi Banerjee, Andrew Y Ng, and Pranav Rajpurkar. 2021. CheXtransfer: Performance and Parameter Efficiency of ImageNet Models for Chest X-Ray Interpretation. *arXiv preprint arXiv:2101.06871* (2021).
- [23] Ishan Misra and Laurens van der Maaten. 2020. Self-supervised learning of pretext-invariant representations. In *Proceedings of the IEEE/CVF Conference on Computer Vision and Pattern Recognition*. 6707–6717.
- [24] Andrew Owens and Alexei A Efros. 2018. Audio-visual scene analysis with self-supervised multisensory features. In *Proceedings of the European Conference on Computer Vision (ECCV)*. 631–648.
- [25] Deepak Pathak, Philipp Krahenbuhl, Jeff Donahue, Trevor Darrell, and Alexei A Efros. 2016. Context encoders: Feature learning by inpainting. In *Proceedings of the IEEE conference on computer vision and pattern recognition*. 2536–2544.
- [26] Alec Radford, Jong Wook Kim, Chris Hallacy, Aditya Ramesh, Gabriel Goh, Sandhini Agarwal, Girish Sastry, Amanda Askell, Pamela Mishkin, Jack Clark, et al. 2021. Learning Transferable Visual Models From Natural Language Supervision. https://cdn.openai.com/papers/Learning_Transferable_Visual_Models_From_Natural_Language_Supervision.pdf.
- [27] Olaf Ronneberger, Philipp Fischer, and Thomas Brox. 2015. U-net: Convolutional networks for biomedical image segmentation. In *International Conference on Medical image computing and computer-assisted intervention*. Springer, 234–241.
- [28] Kihyuk Sohn, Chun-Liang Li, Jinsung Yoon, Minh Jin, and Tomas Pfister. 2020. Learning and Evaluating Representations for Deep One-class Classification. *arXiv preprint arXiv:2011.02578* (2020).
- [29] Marco Tagliasacchi, Beat Gfeller, Félix de Chaumont Quitry, and Dominik Roblek. 2019. Self-supervised audio representation learning for mobile devices. *arXiv preprint arXiv:1905.11796* (2019).
- [30] Aiham Taleb, Christoph Lippert, Tassilo Klein, and Moin Nabi. 2019. Multimodal self-supervised learning for medical image analysis. *arXiv preprint arXiv:1912.05396* (2019).

- [31] Aiham Taleb, Winfried Loetzsch, Noel Danz, Julius Severin, Thomas Gaertner, Benjamin Bergner, and Christoph Lippert. 2020. 3D Self-Supervised Methods for Medical Imaging. *arXiv preprint arXiv:2006.03829* (2020).
- [32] Yonglong Tian, Yue Wang, Dilip Krishnan, Joshua B Tenenbaum, and Phillip Isola. 2020. Rethinking few-shot image classification: a good embedding is all you need? *arXiv preprint arXiv:2003.11539* (2020).
- [33] Xiu-Shen Wei, Jianxin Wu, and Quan Cui. 2019. Deep learning for fine-grained image analysis: A survey. *arXiv preprint arXiv:1907.03069* (2019).
- [34] RA Welikala, Jamshid Dehmeshki, Andreas Hoppe, V Tah, S Mann, Thomas H Williamson, and SA Barman. 2014. Automated detection of proliferative diabetic retinopathy using a modified line operator and dual classification. *Computer methods and programs in biomedicine* 114, 3 (2014), 247–261.
- [35] Roshan A Welikala, Muhammad Moazam Fraz, Jamshid Dehmeshki, Andreas Hoppe, V Tah, S Mann, Thomas H Williamson, and Sarah A Barman. 2015. Genetic algorithm based feature selection combined with dual classification for the automated detection of proliferative diabetic retinopathy. *Computerized Medical Imaging and Graphics* 43 (2015), 64–77.
- [36] Steffen Wolf, Fred A Hamprecht, Jan Funke, HHMI Janelia, and VA Ashburn. 2020. Inpainting Networks Learn to Separate Cells in Microscopy Images. In *The British Machine Vision Conference (BMVC)*.
- [37] Richard Zhang, Phillip Isola, and Alexei A Efros. 2016. Colorful image colorization. In *European conference on computer vision*. Springer, 649–666.
- [38] Zongwei Zhou, Vatsal Sodha, Md Mahfuzur Rahman Siddiquee, Ruibin Feng, Nima Tajbakhsh, Michael B Gotway, and Jianming Liang. 2019. Models genesis: Generic autodidactic models for 3d medical image analysis. In *International Conference on Medical Image Computing and Computer-Assisted Intervention*. Springer, 384–393.